https://doi.org/10.33263/Materials22.250255

ISSN: 2668-5728 https://materials.international

Materials International

Volume 2, Issue 2, Pages 0250-0255
2020

Received: 02.05.2020
Accepted: 22.05.2020
Published: 25.05.2020

Article

Development of Fe/Ru Bimetallic Nanoparticles for Promising Application in the Selective Synthesis of SWNTs

Pradeep Kumar Khiriya[1], Meet A. Moradiya[1], Purnima Swarup Khare[1,*]

[1] School of Nanotechnology, Rajiv Gandhi Proudyogiki Vishwavidyalaya, Bhopal, Madhya Pradesh, India
* Correspondence: purnima.swaroop@rgtu.net; Scopus ID: 55850045100

Abstract: Fe/Ru nanoparticles were synthesized using a modified chemical reduction under hydrothermal reaction and PAA as a protective agent, to product uniform Fe/Ru bimetallic nanoparticles. The as-synthesized bimetallic nanoparticles were characterized by Transmission Electron Microscope (TEM), X-Ray Photon Spectroscopy (XPS), and UV-Visible spectroscopy. The synthesized Fe/Ru bimetallic nanoparticles possess uniform growth as well as high surface area. The results suggest that the proposed Fe/Ru bimetallic nanoparticles could be utilized as a catalyst for the surface growth of SWNTs by chemical vapor deposition (CVD).

Keywords: Fe/Ru bimetallic Nanoparticles; Catalyst, SWNTs.

1. Introduction

The design and controlled synthesis of nanostructured materials with functional properties have attracted significant interest due to their diverse applications such as magnetic devices, catalysts, optoelectronics, and single-electron transistors [1-3].

Bimetallic nanoparticles, composed of two different metals, have drawn a greater interest than the monometallic [4, 5]. Constituting metals and their nanometric size determine the properties of the bimetallic nanoparticles. These are synthesized by the combination of different architectures of metallic nanoparticles [6]. Researchers have recently focused on the selective preparation of new bimetallic nanoparticles in various forms, such as alloys, a core-shell, and a contact aggregate, as they may have unique electronic, optical and catalytic properties, absent from nanoparticles, corresponding monometallic compounds [7-10]. The synthesis method determines the structure and miscibility of the two metals in bimetallic nanoparticles.

The Fe/Ru bimetallic nanoparticles were subsequently loaded onto a $MgAl_2O_4$ supporter with K_2O as promoters and used as a catalyst for water-gas shifts reaction. In contrast, the Fe/Ru bimetallic nanoparticles show high catalytic activity for water-gas shift reaction [11]. For example, in the case of a Fe/Co-Zeolite system with camphor, the ideal temperature for SWNTS growth was reported

Cite This Article: Khiriya, P.K.; Moradiya, M.A.; Khare, P.S.Development of Fe/Ru Bimetallic Nanoparticles for Promising Application in the Selective Synthesis of SWNTs. Mat Int **2020**, 2, 0250-0255. https://doi.org/10.33263/Materials22.250255

to be around 900°C, whereas, for MWCNTs, the ideal growth temperature was reported to be 650°C [12]. Bilu Liu reported that the novel bimetallic nanoparticles of Co/Pt catalyst for the very selective growth of excellent quality SWNTSs with a narrow chirality distribution at relatively high temperatures of 800°C and 850°C using atmospheric pressure CVD (APCVD) [13]. S.Y. Moon et al. reported the evolution of CNT fiber synthesis with Fe/Ni-based NPs in the gas phase during CVD [14]. A. Castan et al. developed a facile synthesis method able to produce a wide range of homogenous bimetallic nanoparticles for efficient catalysts for SWNTS growth with a good yield and small diameter [15]. Xuan Wang demonstrated that bimetallic catalysts such as Fe/Ru and Fe/Pt in size range of 0.5-3 nm are currently being considered for the effective growth of SWNTs on flat surfaces [16].

In this study, we report an efficient synthesis route to achieve Fe/Ru bimetallic nanoparticles using modified chemical reduction under the hydrothermal method to reduce the mixture of iron and ruthenium chloride in the presence of PAA. We proposed Fe/Ru bimetallic nanoparticles could be utilized as a catalyst for the surface growth of SWNTs by chemical vapor deposition.

2. Materials and Methods

Analytical-grade reagents of Iron chloride tetrahydrate ($FeCl_3 \cdot 4H_2O$), Ruthenium chloride hydrate ($RuCl_3 \cdot nH_2O$), Poly (acrylic acid, sodium salt) 35 wt% solution in water (Mw, 15,000), NaOH and double distilled water were used in all experiments. All the chemicals were used as received without further purification.

A typical procedure is described as follows. Firstly, We prepared two samples with the different molar ratio now each sample contain 0.4050 gm of $FeCl_3.6H_2O$, 0.9315 gm of $RuCl_3.nH_2O$ gm, 0.9779 gm of PAA and 0.405 gm of $FeCl_3.6H_2O$, 1.242 gm of $RuCl_3.nH_2O$, 1.22 gm of PAA were dissolved 45 ml double distilled water in two separate bickers and magnetically stirred vigorously for 45 min. After that, 0.1 M of sodium hydroxide was mixed. Then the combined solution was transferred into 50 ml of Teflon cup in a stainless steel-lined autoclave. The autoclave was heated at 80°C for 3h, and the mixer was cooled to room temperature by removing the heat source. The nanoparticles were separated from the mixture by ultrasonication for 1.5 h. After removing the supernatant, the precipitate was rinsed with methanol and centrifuged at 5000 rpm for 15 min several times. Finally, these clean precipitates were dried in an oven overnight in the air at 50°C. A series of bimetallic nanoparticles were prepared by varying the molar ratio of iron to ruthenium precursors.

3. Results and Discussion

3.1. Morphological surface analysis.

Transmission electron microscopy (TEM) used to analyze the structure and composition of Fe/Ru bimetallic nanoparticles. The TEM image patterns of the as-synthesized two Fe/Ru nanoparticles samples are shown in Fig. 1(a,b). The formation of bimetallic nanoparticles was first confirmed by TEM. The molar ratio of iron chloride to ruthenium chloride precursor contained in the reactant solution was 1:3 and 1:4, and PAA to metal chloride precursor ratio is fixed 5:1 in both samples. The Fe/Ru (1:3) nanoparticles are more uniform and spherical as compared with Fe/Ru (1:4). Although the sample preparation for TEM is performed inside a glove box, the samples are transiently exposed to air when mounting samples on the microscope. Therefore, a thin oxide-layer on these nanoparticles in unavoidable. Besides, in the upper right region of Fig. 1, the selected area electron diffraction (SAED) pattern of the bimetallic Fe/Ru bimetallic nanoparticles is represented. Both SAED patterns did not show many spots and circles, indicating that the bimetallic Fe/Ru nanoparticles are very fine particles. High-Resolution transmission electron microscopy (HRTEM) was used to analyze the structure and composition of Fe/Ru bimetallic nanoparticles. When the molar ratio of iron to ruthenium is 1:3, it is found that the average size of the nanoparticles is ~5 nm are observed, as showed in figure 2(A). When the molar ratio has increased to 1:4, it is clearly seen that most of the nanoparticles are in larger diameter with an average of ~11 nm diameter in figure 2(B).

Figure 3(A, B) shows the typical HRTEM image of two bimetallic nanoparticles with a

different molar ratio of iron to the ruthenium precursor. Judging from the surface plot profile, the Fe/Ru (1:3) bimetallic nanoparticles appeared to be single crystalline nature and spherical as compared to Fe/Ru (1:4). Jian-Quan Du et al. reported it is difficult to obtain homogeneous bimetallic nanoparticles when the Fe/Ru molar ratio is too high [11].

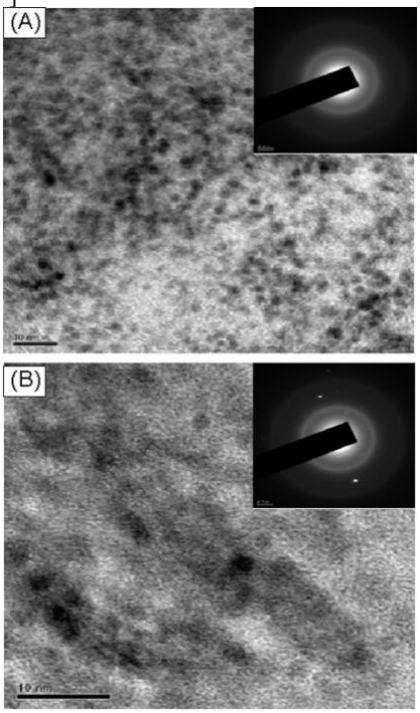

Figure 1. The representative transmission electron microscope (TEM) micrographs and the selected area electron diffraction (SAED) patterns different from the molar ratio of (a)1:3; (b) 1:4.

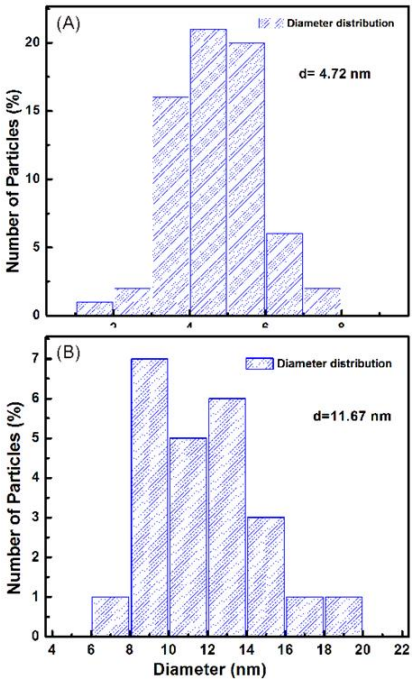

Figure 2. The histogram of as-prepared Fe/Ru bimetallic nanoparticles with different molar ratios (a) 1:3; (b) 1:4.

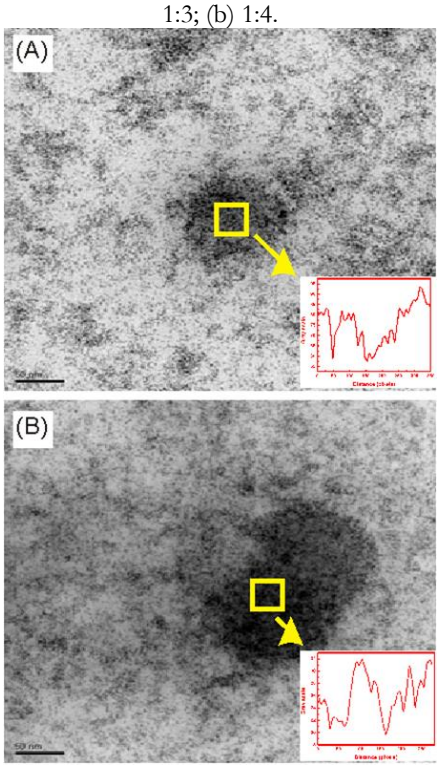

Figure 3. Typical high-resolution TEM images of Fe/Ru alloys nanoparticles with Fe/Ru molar ratio are 1:3 and 1:4, as well as the molar ratio of PAA to metal ions for all is 5:1, while the inset shows the surface plot profile of selected parts.

3.2. X-ray Photoelectron Spectroscopy (XPS) Surface Analysis.

To analyze the chemical state of the particles to be created in the Ferric chloride and Ruthenium trichloride reactant solution assisted by hydrothermal process, the X-ray Photon Spectroscopy (XPS) was used and the results attained from the examination are represented in Fig. 4. The similar surface element states can be observed in the samples prepared with a different molar ratio of iron to ruthenium precursors. Figure 3a depicts that two ion elements in the 2p region with $Fe_{3/2}$ at approximately 706.0 eV and Fe $2p_{1/2}$ at approximately 719.5 eV are observed for two samples (1:3 and 1:4) indicating a pure metallic state of Fe atoms [17]. The other two characteristic peaks observed with Fe $2p_{1/2}$ at about 723.5 eV and Fe $2p_{3/2}$ at about 709.5 eV for the samples prepared in the aqueous solution without NaOH addition demonstrate the formation iron oxides of Fe_3O_4 [18]. While for the samples prepared with NaOH water solvent, the peak intensity corresponding to metallic Fe is much stronger, indicating that slighter

oxidization occurs on the surface of the samples [19]. Figure 4(B) shows that the ruthenium in the 3p region. The peaks of 3p3/2 ruthenium were observed from each level of 462.0 eV and 463.8 eV, and peaks of 3p1/2 ruthenium were identified from each point of 484.1 eV and 486.0 eV. Thus, based on these results, the contemporaneous synthesis of metallic Ru was identified [20, 21]. From the results obtained by the XPS analysis, the particles synthesized by the chemical reduction assisted hydrothermal process employed in this study were identified as the bimetallic Fe/Ru nanoparticles, which were comprised of metallic iron and metallic ruthenium.

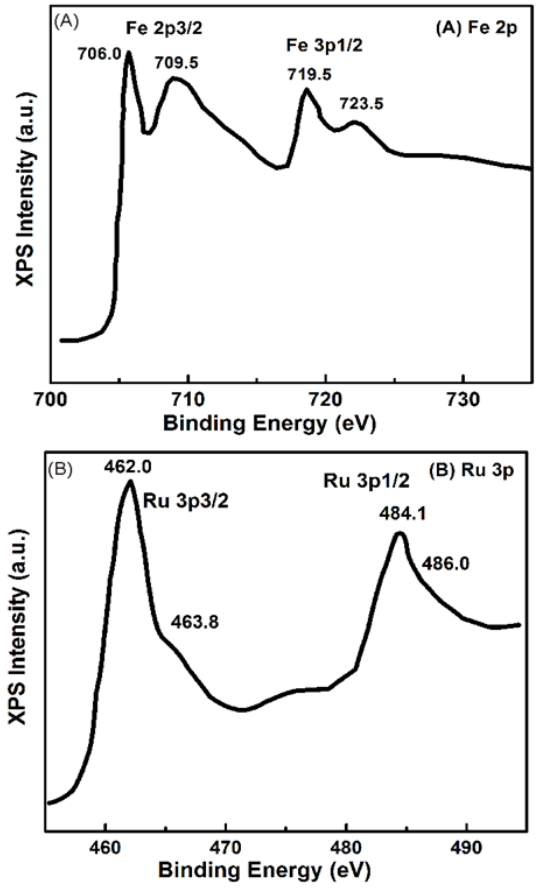

Figure 4. XPS spectra of bimetallic Fe/Ru nanoparticles prepared with different iron to ruthenium molar ratio of (a) 1:3 and (b) 1:4.

3.3. UV-Visible spectroscopy.

An absorption spectrophotometer works in a range from about 200 nm (in the near ultra-violet) to about 800 nm (in the very near infra-red), as defined by the working range of typical commercial UV-VIS spectrophotometers. Figure 5 depicts that there is no significant surface plasmon resonance (SPR) absorption peaks were present in the blank glass in the scanned wavelength range.

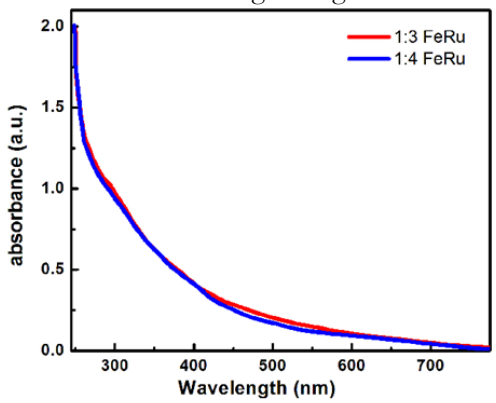

Figure 5. UV-Visible spectra of bimetallic Fe/Ru nanoparticles prepared with different iron to ruthenium molar ratio of (a) 1:3 and (b) 1:4.

3.4. Development of CNTs.

Chemical vapor deposition (CVD) is commonly referred to as catalytic chemical vapor deposition (c-CVD) due to the use of metal catalysts in the thermal decomposition of a hydrocarbon vapor. Catalysts play a very significant role in the growth of CNTs [22]. An ideal catalyst material should be mono-dispersed on the surface of the substrate and offer high surface area as well as controlled growth of CNTs with better diameter distribution [23]. By increasing the interactions between catalyst support and the catalyst nanoparticles, it is possible to control some of the problems encountered at high temperatures. Hydrocarbon sources may be benzene, alcohol, carbon monoxide, and camphor [24]. For the decomposition of hydrocarbons, nanoscale transition metal catalysts such as Fe, Co, Ni, Mo, Ru, Cu, Au, Ag, and Pt are commonly used, but in some cases, metal catalysts are mixed with catalyst supports such as SiO_2, MgO and Al_2O_3 in order to increase the surface area of the catalytic reaction [25-27]. The bimetallic nanoparticles based catalysts are compared with single metal catalysts such as Fe, Ru, and Pt of similar size, bimetallic catalyst Fe/Pt improved the production of SWNTSs by at least 200% [16].

It has been reported that the nanoparticles of Fe, Ru, and Pt are active towards the decomposition of methane and are capable of dissolving carbon atoms [16]. However, for Pt nanoparticles, judged from the phase diagram of Pt and C, a temperature higher than 1500°C is probably required to precipitate carbon from the Pt-C alloy [28]. Thus,

under our reaction temperature of 900°C, single Pt nanoparticles incapable of precipitating carbon atoms showed no activity toward the SWNT growth. Possible reasons for the synergistic effect of Ru or Pt when alloyed with iron may be elicited from three aspects: first, the enhanced ability of bimetallic nanoparticles in decomposing methane and in dissolving carbon atoms; second, the improved wetting ability of bimetallic nanoparticles on SiO_2 surface; third, the stronger binding energy between bimetallic nanoparticles and graphene sheets for the formation of graphene caps [28]. Thus the present work offers a simple chemical way of producing Fe/Ru nanoparticles and proposed application of the efficient and reproducible surface growth of SWNTs.

4. Conclusions

In this study, the Fe/Ru alloys bimetallic nanoparticles have been synthesized by modified chemical reduction associated with the hydrothermal method, to obtain bimetallic nanoparticles such as Fe/Ru (1:3) and Fe/Ru (1:4) alloys in the size distribution of 2-6 nm. The TEM indicates that the synthesized nanoparticles are uniform and spherical in nature. The TEM image of the molar ratio of 1:3 shows the very low agglomeration, uniform size distribution, and high growth rate as compared to the molar ratio of 1:4. The XPS data of as-synthesized Fe/Ru alloys bimetallic nanoparticles shows the existence of Fe metal, and metallic Ru (RuO) was identified. The UV-Visible data indicates that there is no significant SPR absorption peaks were present in the scanned wavelength range. The results suggest that the proposed Fe/Ru bimetallic nanoparticles could be utilized as a catalyst for the surface growth of SWNTs by chemical vapor deposition (CVD).

Funding

This research received no external funding.

Acknowledgments

The authors declare no acknowledgments.

Conflicts of Interest

The authors declare no conflict of interest.

References

1. Rana, B.; Otani, Y.C. Towards Magnonic Devices Based on Voltage-Controlled Magnetic Anisotropy. *Commuication Physics* **2019**, *2*, 1–12, https://doi.org/10.1038/s42005-019-0189-6.
2. Srinoi, P.; Chen, Y.T.; Vittur, V.; Marquez, M.D.; Lee, T.R. Bimetallic Nanoparticles: Enhanced Magnetic and Optical Properties for Emerging Biological Applications. *Applied Sciences* **2018**,*8*, https://doi.org/10.3390/app8071106.
3. Korgaokar, S.; Moradiya, M.; Prajapati, O.; Thakkar, P.; Pala, J.; Savaliya, C.; Parikh, S.; Markna, J. H. Highly Sensitive Nanostructure SnO2 based Gas Sensor for Environmental Pollutants. *AIP Conference Proceedings***2017**, *1837*, https://doi.org/10.1063/1.4982134.
4. Hajipour, A.R.; Khorsandi, Z.; Farrokhpour, H. In Situ Synthesis of Carbon Nanotube-Encapsulated Cobalt Nanoparticles by a Novel and Simple Chemical Treatment Process: Efficient and Green Catalysts for the Heck Reaction. *New Journal Chemistry***2019**, *43*, 8215–8219, https://doi.org/10.1039/c9nj00813f.
5. Harikumar, P.S.; Hridya, T.K. Application of CuNi Bimetallic Nanoparticle as an Adsorbent for the Removal of Heavy Metals from Aqueous Solution.*International Journal of Environmental Analytical Chemistry* **2019**, *00*, 1–15, https://doi.org/10.1080/03067319.2019.1673383.
6. Loza, K.; Heggen, M.; Epple, M. Synthesis, Structure, Properties, and Applications of Bimetallic Nanoparticles of Noble Metals. *Advanced Functional Materials***2020**, https://doi.org/10.1002/adfm.201909260.
7. Kumari, N.; Kour, S.; Singh, G.; Chauhan, A.; Verma, R.; Sharma, R.K. A Brief Review on the Synthesis of Bimetallic Nanoparticles for Biomedical and Solar Energy Applications. *AIP Conference Proceedings* **2020**, *2220,*https://doi.org/10.1063/5.0001320.
8. Moradiya, M.A.; Dangodara, A.; Pala, J.; Savaliya, C.R.; Dhruv, D.; Rathod, V.R.; Joshi, A.D.; Shah, N.A.; Pandya, D.; Markna, J.H. A natural tomato slurry as a photosensitizer for dye-sensitized solar cells with TiO2/CuO composite thin films. *Separation Science and Technology* **2019**, *54*, 207-212,https://doi.org/10.1080/01496395.2018.1444053.
9. Khanna, S; Islam, N. Carbon Nanotubes-Properties and Applications. *Organic and Medicinal Chemistry* 2018, 7, http://dx.doi.org/10.19080/OMCIJ.2018.07.555705.

10. Jiang, X.; Fan, X.; Xu, W.; Zhang, R.; Wu, G. Biosynthesis of Bimetallic Au-Ag Nanoparticles Using Escherichia Coli and Its Biomedical Applications. *ACS Biomaterial Scienceand Engineering* **2019**, *6,* 680-689, https://doi.org/10.1021/acsbiomaterials.9b01297.
11. Du, J.Q.; Zhang, Y.; Tian, T.; Yan, S.C.; Wang, H.T. Microwave Irradiation Assisted Rapid Synthesis of Fe-Ru Bimetallic Nanoparticles and Their Catalytic Properties in Water-Gas Shift Reaction. *Materials Research Bulletin* **2009**, *44*, 1347–1351, https://doi.org/10.1016/j.materresbull.2008.12.001.
12. Kumar, M.; Ando, Y. Chemical Vapor Deposition of Carbon Nanotubes: A Review on Growth Mechanism and Mass Production. *Journal of Nanoscience and Nanotechnology* **2010**, *10*, 3739–3758, https://doi.org/10.1166/jnn.2010.2939.
13. Liu, B.; Ren, W.; Li, S.; Liu, C.; Cheng, H.M. High Temperature Selective Growth of Single-Walled Carbon Nanotubes with a Narrow Chirality Distribution from a CoPt Bimetallic Catalyst. *Chemical Communication***2012**, *48*, 2409–2411, https://doi.org/10.1039/c2cc16491d.
14. MOON, S.; Kim, W.S. The Synergetic Effect of Bimetallic Catalyst for the Synthesis of Carbon Nanotube Aerogels and Their Predominant Chirality. *Chemistry - A European Journal***2019**, *25*,https://doi.org/10.1002/chem.201903273.
15. Castan, A.; Forel, S.; Catala, L.; Florea, I.; Fossard, F.; Bouanis, F.; Andrieux-Ledier, A.; Mazerat, S.; Mallah, T.; Huc, V.; Loiseau, A.; Cojocaru, C.S. New Method for the Growth of Single-Walled Carbon Nanotubes from Bimetallic Nanoalloy Catalysts Based on Prussian Blue Analog Precursors. *Carbon* **2017**, *123*, 583–592, https://doi.org/10.1016/j.carbon.2017.07.058.
16. Wang, X.; Yue, W.; He, M.; Liu, M.; Zhang, J.; Liu, Z. Bimetallic Catalysts for the Efficient Growth of SWNTs on Surfaces. *Chemical Mateials.***2004**, *16*, 799–805, https://doi.org/10.1021/cm035070u.
17. Yang, X.Y.; Yang, B.; Li, X.P.; Cao, Y.; Yu, R.H. Structural-Controlled Chemical Synthesis of Nanosized Amorphous Fe Particles and Their Improved Performances. *Journal of Alloys Compound***2015**, *651*, 551–556, https://doi.org/10.1016/j.jallcom.2015.08.156.
18. Yamashita, T.; Hayes, P. Analysis of XPS Spectra of Fe 2+ and Fe 3+ Ions in Oxide Materials. *Applied surface science.***2008**, *254*, 2441–2449, https://doi.org/10.1016/j.apsusc.2007.09.063.
19. Gota, S.; Guiot, E.; Henriot, M.; Gautier-Soyer, M. Atomic-Oxygen-Assisted MBE Growth of α −Fe2 O3 on α −Al2 O3 (0001): Metastable FeO(111)-like Phase at Subnanometer Thicknesses. *Physical Review B***1999**, *60*, 14387–14395, https://doi.org/10.1103/physrevb.60.14387.
20. Bensebaa, F.; Patrito, N.; Le Page, Y.; L'Ecuyer, P.; Wang, D. Tunable Platinum-Ruthenium Nanoparticle Properties Using Microwave Synthesis. *Journal of material chemistry* **2004**, *14*, 3378–3384, https://doi.org/10.1039/b404280h.
21. Morgan, D.J. Resolving Ruthenium: XPS Studies of Common Ruthenium Materials. *Surface and Interface Analysis* **2015**, *47*, 1072–1079, https://doi.org/10.1002/sia.5852.
22. Latorre, N.; Romeo, E.; Cazaña, F.; Ubieto, T.; Royo, C.; Villacampa, J.I.; Monzón, A. Carbon Nanotube Growth by Catalytic Chemical Vapor Deposition: A Phenomenological Kinetic Model. *Journal of Physical Chemistry C***2010**, *114*, 4773–4782,https://doi.org/10.1021/jp906893m.
23. Hoyos-Palacio, L.M.; García, A.G.; Pérez-Robles, J.F.; González, J.; Martínez-Tejada, H.V. Catalytic Effect of Fe, Ni, Co and Mo on the CNTs Production. *IOP Conference Series: Materials Science and Engineering***2014**, *59*, https://doi.org/10.1088/1757-899X/59/1/012005.
24. Ando, Y.; Zhao, X.; Sugai, T.; Kumar, M. Growing carbon nanotubes. **2004**, No. October, 22–29.
25. Dupuis, A.C. The Catalyst in the CCVD of Carbon Nanotubes-a Review. *Progress in Materials Science***2005**, *50*, 929–961, https://doi.org/10.1016/j.pmatsci.2005.04.003.
26. Varshney, D.; Weiner, B.R.; Morell, G. Growth and Field Emission Study of a Monolithic Carbon Nanotube/Diamond Composite. *Carbon***2010**, *48*, 3353–3358, https://doi.org/10.1016/j.carbon.2010.05.025.
27. Shen, W.; Li, F.; Liu, C.; Yin, L.C. Changing the Chirality of Single-Wall Carbon Nanotubes during Epitaxial Growth: A Density Functional Theory Study. *New Carbon Material***2016**, *31*, 525–531, https://doi.org/10.1016/S1872-5805(16)60030-6.
28. Moisala, A.; Nasibulin, A.G.; Kauppinen, E.I. The Role of Metal Nanoparticles in the Catalytic Production of Single-Walled Carbon Nanotubes - A Review. *Journal of Physics: Condensed Matter***2003**, *15*, https://doi.org/10.1088/0953-8984/15/42/003.